Pharmaceutical Research, Vol. 24, No. 8, August 2007 (© 2007)
DOI: 10.1007/s11095-007-9259-7

Research Paper

Engineered Polyallylamine Nanoparticles for Efficient *In Vitro* Transfection

Atul Pathak,[1] Anita Aggarwal,[1] Raj K. Kurupati,[1] Soma Patnaik,[1] Archana Swami,[1] Yogendra Singh,[1] Pradeep Kumar,[1] Suresh P. Vyas,[2] and Kailash C. Gupta[1,3]

Received August 19, 2006; accepted January 31, 2007; published online March 24, 2007

Purpose. Cationic polymers (i.e. polyallylamine, poly-L-lysine) having primary amino groups are poor transfection agents and possess high cytotoxicity index when used without any chemical modification and usually entail specific receptor mediated endocytosis or lysosomotropic agents to execute efficient gene delivery. In this report, primary amino groups of polyallylamine (PAA, 17 kDa) were substituted with imidazolyl functions, which are presumed to enhance endosomal release, and thus enhance its gene delivery efficiency and eliminate the requirement of external lysosomotropic agents. Further, systems were cross-linked with polyethylene glycol (PEG) to prepare PAA-IAA-PEG (PIP) nanoparticles and evaluated them in various model cell lines.

Materials and Methods. The efficacy of PIP nanoparticles in delivering a plasmid encoding enhanced green fluorescent protein (EGFP) gene was assessed in COS-1, N2a and HEK293 cell lines, while their cytotoxicity was investigated in COS-1 and HEK293 cell lines. The PAA was chemically modified using imidazolyl moieties and ionically cross-linked with PEG to engineer nanoparticles. The extent of substitution was determined by ninhydrin method. The PIP nanoparticles were further characterized by measuring the particle size (dynamic light scattering and transmission electron microscopy), surface charge (zeta potential), DNA accessibility and buffering capacity. The cytotoxicity was examined using the MTT method.

Results. *In vitro* transfection efficiency of synthesized nanoparticles is increased up to several folds compared to native polymer even in the presence of serum, while maintaining the cell viability over 100% in COS-1 cells. Nanoparticles possess positive zeta potential between 5.6–13 mV and size range of 185–230 nm in water. The accessibility experiment demonstrated that nanoparticles with higher degree of imidazolyl substitution formed relatively loose complexes with DNA. An acid-base titration showed enhanced buffering capacity of modified PAA.

Conclusions. The PIP nanoparticles reveal tremendous potential as novel delivery system for achieving improved transfection efficiency, while keeping the cells at ease.

KEY WORDS: buffering capacity; DNA accessibility; GFP; imidazole acetic acid; nanoparticles; polyallylamine; transfection.

INTRODUCTION

The fundamental aim of molecular medicine is to fabricate novel therapeutic options (nucleotide based macromolecules) allowing treatment at the level of genes, involved in pathophysiology of diseases. Indeed, gene therapy is an emerging way of correcting genetic disorders at their molecular roots, redefining and revolutionizing the practice of medicine in near future (1). Clinical use of these therapeutic agents is severely hampered by lack of appropriate carrier system that helps DNA in reaching the target cells and in the subsequent intracellular trafficking (2). So far, various viral carrier systems, such as retrovirus (3,4), adenovirus (5,6); and non-viral like cationic lipids (7,8), liposomes (9), nanoparticles have been exploited for this purpose (10). In spite of natural ability of viruses to infect host cells, risk of immunogenicity, random integration of vector DNA into host chromosome, their recombination with wild type viruses and toxicity are associated problems that make non-viral gene delivery systems the vector of choice in gene therapy (11–13). A variety of polycations have been shown to be competent in DNA delivery such as polyethylenimine (PEI), poly(L-lysine) (PLL), polyamidoamine (PAMAM) dendrimers and poly (2-dimethyl amino ethyl) methacrylate (PDMAEMA) etc. Among all these, PEI is the most extensively studied polymer because it efficiently condenses DNA and the resulting PEI/DNA complex can act as proton sponge, thus enabling DNA delivery into cytoplasm by rupturing endosomes. Behr introduced the concept of "proton sponge" and hypothesized that polymers with buffering capacity between pH 5.0–7.2 such as PEI and imidazole containing polymers buffer the endosome and potentially induce its rupture (14). This endosome buffering not only inhibits the degradative enzymes (which perform optimally

[1] Institute of Genomics and Integrative Biology, Delhi University Campus, Mall Road, Delhi 110007, India.
[2] Department of Pharmaceutical Sciences, Dr. Harisingh Gour University, Sagar 470003, M.P., India.
[3] To whom correspondence should be addressed. (e-mail: kcgupta@igib.res.in)

within acidic pH ambience of the endolysosome compartments), but also induces stronger electrostatic repulsion among protonated head groups of cationic systems, leading to osmotic swelling and eventual endosome bursting. However, the clinical development of PEIs has been sluggish due to molecular heterogeneity and acute toxicity (15,16).

Recently, polyallylamine (PAA), a synthetic cationic polymer, which possesses high density of primary amino groups, exists as free amino or as cationic ammonium salt, has drawn considerable attention as a non-viral gene delivery system (17,18). PAA carries a strong positive charge, which makes it suitable to bind and package negatively charged DNA. It is a pH-sensitive polymer, extensively used in the pharmaceutical industry. However, cytotoxicity of PAA, owing to its strong polycationic character, has severely restricted its use as a gene delivery system. In order to reduce its cytotoxicity, Boussif *et al.* modified PAA with hydrophilic methyl glycolates and found that its ability to mediate gene transfer into cells increased by several order of magnitude (18), while decreasing cytotoxicity at the same time. Cytotoxicity of polycations like PEI and PLL has also been reduced by introducing various modifications with pegylation (19–21), acetylation (22), grafting with dextran and cyclodextrin (23,24). These chemical modifications not only decrease cytotoxicity but also enhance transfection efficiency. Inefficient release of complexes from endocytic vesicles into the cytoplasm leads to poor gene delivery. Like PLL, PAA also contains non-titratable primary amino groups and lacks titratable secondary and tertiary amino function, which contributes to the buffering capacity. Hence, osmotic endosomal swelling is not induced by these polymers, leading to feeble DNA-polymer complex escape (18,25). To overcome this obstacle, addition of lysosomotropic agents, such as chloroquine is required to facilitate the escape from endosome, which limits its *in vivo* applications. More recently, it has been reported that imidazolyl moiety, by virtue of its proton sponge property, improves transfection efficiency of polycations like PLL, PEI and chitosan (25–29). The weakly basic imidazolyl group with pKa being within the acidic range of endosome lumen (pH 5.5–6.5) acts as proton sponge inside the endosome compartment. Imidazole containing polymers were designed by incorporating the residue of histidine, which enhances the release of the DNA-polymer complex into the cytoplasm by virtue of its proton sponge property following endocytosis. Recently, imidazolyl-PEI nanoparticles have been investigated in the authors' laboratory as efficient gene delivery system (30). In spite of having well spaced primary amino groups, the low proton affinity of PAA is well documented and the polymer is predicted to exist like micelles in aqueous solutions with separate hydrophobic and hydrophilic domains (31). Moreover, micelle forming lipoamines have been shown to be more efficacious in gene delivery (32). The properties of PAA can be well utilized for designing the transfection agents, as primary amino groups can be readily substituted chemically by various groups.

In a quest to develop effective gene delivery system, the current study has been designed to reduce the cytotoxicity and improve transfection efficiency of PAA by substituting primary amino groups with imidazolyl moieties, which form relatively loose complexes with DNA. Later, the imidazolylated PAA was converted into nanoparticles by using a homobifunctional PEG cross-linker. We explored PAA based nanoparticles as DNA delivery system on COS-1, N2a and HEK293 cell lines, without addition of external lysosomotropic agent. The transfection efficiency of nanoparticles improved markedly over native PAA.

MATERIALS AND METHODS

Materials, Expression Systems and Cell Cultures

PAA (MW 17 kDa), PEI (25 kDa, branched), 4-imidazole acetic acid hydrochloride (IAA-HCl), 3-(4,5-dimethylthiazol-2-yl)-2,5-diphenyltetrazolium bromide (MTT), agarose, Tris, HEPES, bromophenol blue (BPB), ethidium bromide (EtBr), 1-ethyl-3-(3-dimethylaminopropyl)carbodiimide (EDAC), xylene cyanol (XC), D_2O and high retention dialysis tubing (cut off 12 kDa) were obtained from Sigma-Aldrich Chemical Co., St. Louis, MO, USA. Polyethylene glycol 6000 (PEG 6000) was procured from Fluka Chemie GmbH, Switzerland. Bradford reagent was purchased from Bio-Rad Inc., Hercules, USA. All other chemicals were of the highest purity and procured locally. All the experiments were carried out using MilliQ (deionized) water, filtered through 0.22-μm sterile filters (Millipore). PEG_{6000}-bis-phosphate was synthesized according to the published protocol from the authors' laboratory (33).

For *in vitro* transfection, mammalian cell line COS-1 (Simian virus 40 transformed kidney cells of an African green monkey), N2a (Mouse neuroblastoma) and HEK 293 (Human embryonic kidney) cell lines were maintained 16 h before the experiments as monolayer cultures in Dulbecco's modified Eagle's culture medium (DMEM) (GIBCO-BRL-Life Technologies, Web Scientific Ltd, UK) supplemented with 10% heat inactivated fetal calf serum (FCS) (GIBCO-BRL Life Technologies) and 50 μg/ml gentamycin. Cultures were maintained at 37°C in a humidified 5% CO_2 atmosphere.

The transfection experiments were performed using the plasmid encoding enhanced green fluorescent protein gene (EGFP) under the cytomegalovirus (CMV) immediate early promoter. The plasmid was transformed into *E. coli* bacterial strain DH5α and extracted from the culture pellets using the Qiagen Maxi-Prep kit (Qiagen S.A., Courtaboeuf, France) as per manufacturer's instructions. The purity and identity of plasmid was confirmed by agarose gel electrophoresis and by the ratio of UV absorbance 260/280 in MilliQ water.

Preparation of PAA-PEG (PP) Nanoparticles

PEG_{6000}-bis (phosphate) (75 mg, 1 mg/ml water) was added dropwise to a stirred solution of PAA (25 mg, 1 mg/ml water) over a period of 45 min to prepare PP nanoparticles (33). The contents of the reaction mixture were stirred overnight, followed by dialysis against water for 72 h with intermittent change of water.

Preparation of Imidazolyl Substituted PAA (PI)

Initially, IAA-HCl (28.6 mg for 10% substitution, 1 mg/ml in dd water) was neutralized by treating it with triethylamine (TEA) (25 μl). The resultant IAA solution was added dropwise to a stirred solution of PAA (25 mg, 1 mg/ml water)

over a period of 30 min. at room temperature. The reaction was further incubated for 1 h at room temperature and subsequently, EDAC (8.5 mg) was added. The reaction mixture was stirred overnight, followed by concentration on a rotary evaporator to reduce the original volume to one third and poured into a dialysis bag. The dialysis was performed against water for 72 h with intermittent change of water, followed by lyophilization. Similarly, 20–90% imidazolyl substituted PI formulations were prepared. PI formulations were characterized by ^{1}H-NMR and FTIR, and the extent of the imidazolyl substitution was determined by ninhydrin method (34,35).

Preparation of PAA-Im-PEG (PIP) Nanoparticles

Nanoparticles of PI were ionically crosslinked with polyethylene glycol$_{6000}$-bis (phosphate) (PBP) (33). In brief, an aqueous solution of PBP (75 mg, 1 mg/ml) was added dropwise to a stirred aqueous solution of PI (25 mg, 1 mg/ml, 10% imidazolyl substituted) over a period of 45 min at room temperature to attain 5% PEG cross-linking. The contents of the reaction mixture were stirred overnight, followed by dialysis against water for 72 h with intermittent change of water. The nanoparticles, thus formed, were lyophilized in a speed vac and then characterized by FTIR, DLS and zeta potential.

Determination of Residual Amino Groups

The imidazolyl content in PI was calculated by ninhydrin method (34,35) with little modification. Briefly, PI (10% imidazolyl substituted, 3 mg) was dissolved in ethylene glycol (1 ml), followed by addition of ninhydrin reagent (4 ml, 5% in ethylene glycol). The reaction mixture was heated at 90°C for 10 min and subsequently, subjected to spectrophotometric estimation of amino groups by ninhydrin method, as reported elsewhere (34,35). Other preparations were also estimated, as described earlier.

Characterization of Nanoparticles

(1) FTIR: Spectra were recorded on a single beam Perkin Elmer (Spectrum BX Series), USA with following scan parameters: scan range: 4,400 – 400 cm^{-1}; number of scans: 16; resolutions: 4.0 cm^{-1}, interval: 1.0 cm^{-1}; unit: %T.
(2) ^{1}H NMR: PI complexes were characterized by ^{1}H-NMR (Bruker Avance, DRX-300, 300 MHz FT-NMR, USA) in D_2O at 25°C.
(3) Measurements of particle size and surface charge: The mean hydrodynamic diameter of nanoparticles was determined by dynamic light scattering (Zetasizer Nano ZS, Malvern Instruments, UK) at fixed angle of 90°at 25°C. All the samples were diluted with fresh MilliQ (deionized) water to ensure light scattering intensity within the required range of the instrument. All the measurements were executed in automatic mode. Average size of each sample was the mean of at least five measurements. The morphology of nanoparticles was observed under transmission electron microscope (TEM) (Fei-Philips Morgagni 268D). The nanoparticle suspension (3 μl) was put on a formvar (polyvinyl formal) coated copper grid and air-dried. Images were recorded in negative mode.

Surface charge on nanoparticles was quantified as zeta potential by laser doppler velocimetry using Zetasizer Nano ZS. Samples were diluted with MilliQ (deionized) water. Zeta potentials were computed from the mean electrophoretic mobility applying the Smoluchowski equation.

Measurement of Buffering Capacity

Acid-base titration was used to determine the buffering capacity of native PAA and PIP nanoparticles (36). The relative buffering capacity of nanoparticles was estimated as amount of protons required for pH change from 9.0 to 3.5 by acid-base titration. In this assay, the samples were prepared by suspending nanoparticles (10 mg/ml) in 150 mM NaCl and adjusted to pH (~9.0) with 1 N NaOH and then the samples were titrated by adding small aliquots (25 μl) of 0.1 M HCl until pH 3.5 is reached.

DNA Accessibility Measurement

PIP nanoparticles in different weight ratios were mixed with DNA (250 μl of 2 μg/ml solution) in Tris buffer (10 mM, pH 7.4) and allowed to incubate for 30 min. Mixture was then stained with 1 μg/ml EtBr in Tris buffer. The fluorescence intensity (A.U.) was measured at an excitation wavelength (λ_{ex}=485 nm) and emission wavelength of 590 nm with a slit width of 5.0 nm (23). A graph was constructed by plotting fluorescence (A.U.) against degree of substitution in nanoparticles.

Gel Retardation Assay

To study the condensation of nanoparticles with DNA, samples at different weight ratios in 5% dextrose solution were electrophoresed on agrose gel. All the samples were incubated for 30 min at room temperature prior to loading on the agarose gel. The nanoparticle-DNA complexes were mixed with loading buffer containing a tracking dye (xylene cyanol) and loaded into individual wells of 0.8% agarose gel and electrophoresed at 100 V for 45 min in TAE buffer (40 mM Tris-HCl, 1% (v/v) acetic acid, 1 mM EDTA). The gels were stained by ethidium bromide and the bands corresponding to plasmid DNA were visualized under a UV transilluminator.

In Vitro Transfection Studies

COS-1 cells were seeded into 96-well plates at a density of 8.0×10^3 cells per well and incubated for 16 h for adherence. After overnight incubation, growth medium was aspirated. GFP reporter gene loaded nanoparticle formulations were diluted with DMEM to a final volume of 80 μl (transfection mixture) and added to the individual wells containing cells. The plate was then incubated at 37°C in a 5% CO_2 humidified atmosphere. After 3 h, transfection mixture was replaced by 200 μl fresh DMEM containing 10% FCS and the cells were incubated for another 36 h. Similarly, transfection studies were

carried out on N2a and HEK293 cell lines. Cells expressing EGFP were visualized under Nikon Eclipse TE 2000-S inverted microscope (Kanagwa, Japan) fitted with C-F1 epifluorescence filter, Ex 450–490, Dichroic mirror DM 505 and barrier filter BA 520. Images were acquired using Nikon digital imaging system. Transfection experiments were repeated five times to check reproducibility of results. Mock treated cells were used as blank.

EGFP Expression Analysis

The total protein expressed was calculated by measuring the fluorescence intensity. After 36 h of addition of transfection mixture, the wells containing cells were washed with PBS (1×50 µl). Thereafter, cells were lysed using 100 µl lysis buffer (10 mM Tris HCl, pH 7.4, 0.5% SDS, and 1 mM EDTA) and incubated at 25°C for 20–25 min. The 20 µl of cell lysate was used to estimate the expressed reporter gene product, green fluorescent protein (GFP), spectrofluorimetrically at an excitation wavelength 488 nm and emission at 509 nm. Background fluorescence and auto fluorescence were determined using mock treated cells. The total recovered cellular protein content in cell lysate from each well was estimated using Bradford reagent by taking BSA as a standard. The amount of protein was estimated from a standard curve. The level of fluorescence intensity of GFP was calculated by subtracting the background values and normalized against protein concentration in cell extracts. The data is presented as arbitrary units (A.U.)/mg of cell protein and results represent mean ± standard deviation for triplicate samples.

Cytotoxicity Studies

The toxicity of PAA and PIP nanoparticles in cell culture was examined by MTT colorimetric assay. Cells were treated similarly, as described in the transfection experiment. The medium was removed and replaced by MTT (0.5 mg dissolved in 1.0 ml of DMEM). The plate was incubated for 30 min at 37°C. The supernatant was aspirated and the formazan crystals were dissolved in 100 µl of isopropanol containing 0.006 M HCl and 0.5% SDS. Aliquots were drawn from each well and the intensity of color was measured spectrophotometrically in an ELISA plate reader (MRX, Dynatech Laboratories) at 540 nm. Untreated cells were taken as control with 100% viability and cells without addition of MTT were used as blank to calibrate the spectrophotometer to zero absorbance. The relative cell viability (%) was calculated by $[\text{abs}]_{\text{sample}}/[\text{abs}]_{\text{control}} \times 100$.

RESULTS

Preparation of PIP Nanoparticles

Cationic polymers (e.g. PLL, PAA) possessing primary amino groups have high cytotoxicity and are inefficient DNA carriers, unless chemically modified or used in presence of lysosomotropic agents. In this study, in order to reduce the cytotoxicity, the amino groups of PAA have been substituted with imidazolyl groups by condensing PAA with 4-imidazole acetic acid (10–90%) in the presence of EDAC. The imidazolyl

Table I. Measurement of Particle Size and Zeta Potential of PIP Nanoparticles

S. No.	Nanoparticle Formulations (17 kDa PAA) (Weight Ratio)	Average Particle Size in nm (PDI)			Zeta Potential (mV)		
		DNA Loaded Nanoparticles (in FCS)	DNA Loaded Nanoparticles (in H_2O)	Nanoparticle (in H_2O)	DNA Loaded Nanoparticles (in FCS)	DNA Loaded Nanoparticles (in H_2O)	Nanoparticle (in H_2O)
1.	PAA (1:0.8)	91.2 (0.908)	291 (0.400)		−3.2	+6.8	+13.8
2.	PP (1:2)	156 (0.636)	211 (0.217)	180 (0.253)	−3.8	+6.3	+13.6
3.	PIP-1 (1:8)	110 (0.697)	208 (0.289)	183 (0.305)	−3.9	+6.1	+13.1
4.	PIP-2 (1:8)	97.1 (0.709)	215 (0.227)	190 (0.283)	−2.8	+5.6	+11.8
5.	PIP-3 (1:8)	141 (0.652)	231 (0.250)	201 (0.313)	−5.5	+5.2	+11.1
6.	PIP-4 (1:8)	157 (0.748)	248 (0.307)	204 (0.325)	−4.4	+4.8	+9.8
7.	PIP-5 (1:8)	163 (0.615)	255 (0.275)	207 (0.343)	−6.1	+4.4	+8.2
8.	PIP-6 (1:8)	136 (0.5.60)	257 (0.186)	210 (0.275)	−5.6	+3.9	+7.7
9.	PIP-7 (1:8)	133 (0.784)	263 (0.258)	216 (0.301)	−7.1	+3.4	+6.5
10.	PIP-8 (1:8)	119 (0.815)	278 (0.257)	220 (0.346)	−7.3	+2.8	+6.1
11.	PIP-9 (1:8)	83 (0.605)	282 (0.235)	228 (0.314)	−7.9	+2.3	+5.6

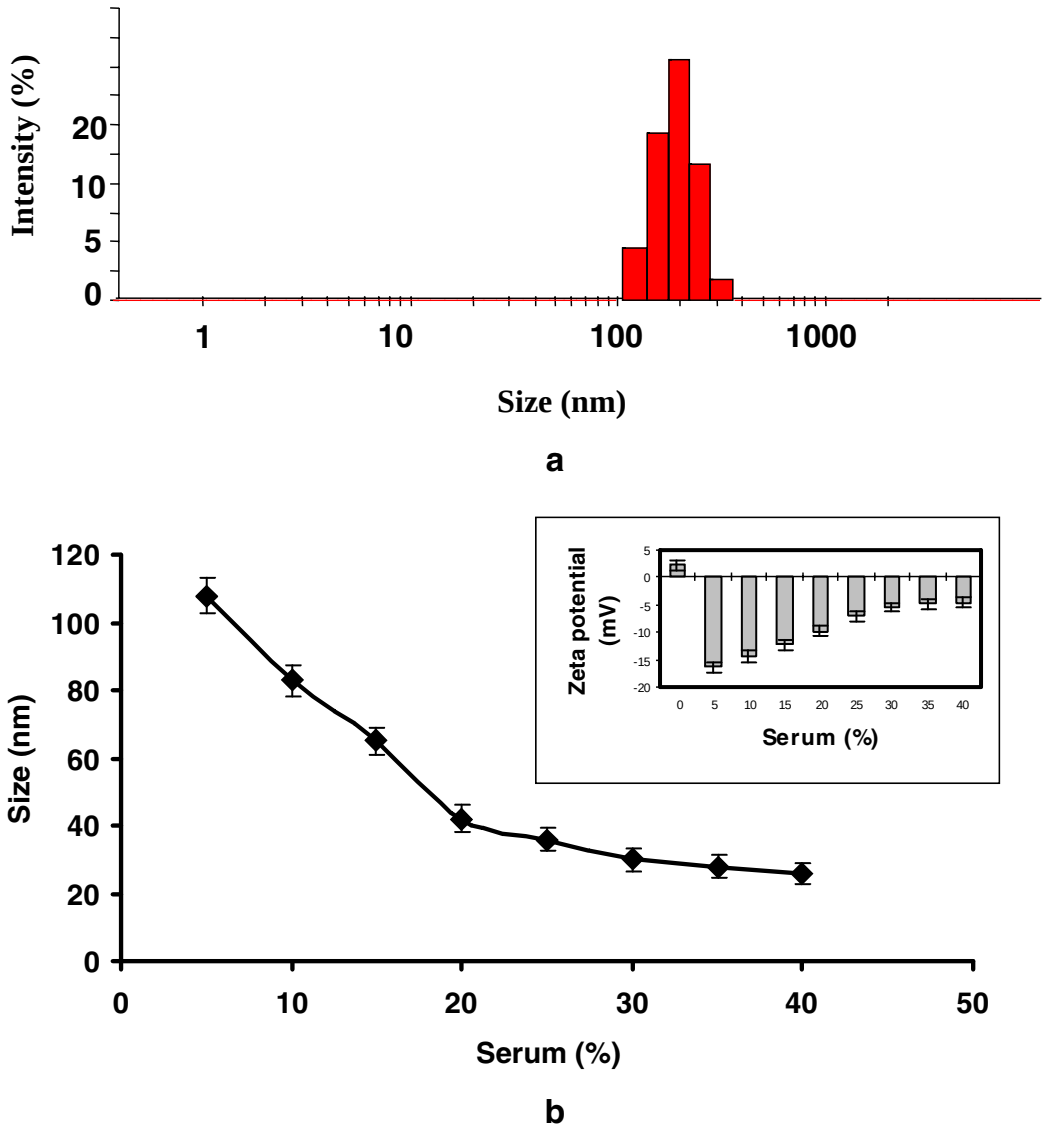

Fig. 1. **a** Schematic representation of dynamic light scattering of PIP-9 nanoparticle formulation. **b** Influence of fetal calf serum (FCS) on PIP-9/DNA complexes size and zeta potential.

content in the resulting PI was determined by ninhydrin assay (34,35), which was found to be 8.2% (PI-10%), 16.1 (PI-20%), 23.5% (PI-30%), 31.1% (PI-40%), 39.5% (PI-50%), 47.3% (PI-60%), 53.8% (PI-70%), 62% (PI-80%), 67.5% (PI-90%). The PI complexes were further characterized by ^{1}H-NMR and FTIR. ^{1}H-NMR (D_2O) δ: 1.22–1.35 (m, -CH_2- and -CH-), 2.5 (d, -NCH_2-), 3.7 (s, -CH_2CO-), 7.22 (s, -CH- Im), 8.5 (s, -CH-Im); IR (KBr) ν: 1630 (*C*=O).

The PI complexes were subsequently cross-linked (5%) with PEG-bis(phosphate) (PBP) to obtain PIP nanoparticles. These were characterized by FTIR, DLS and zeta potential. The peaks at 1,281 and 1,105 cm^{-1} in PIP nanoparticles correspond to C-O (ether) twisting and stretching frequencies, respectively.

Particle Size and Surface Charge

The particle size of all nanoparticle formulations was found to be in the range of 180–230 nm (Table I) with polydispersity index (PDI) lower than 0.35, indicating a narrow size distribution. The particle size distribution pattern indicated that all particles were of nanometer size and devoid of aggregates (Fig. 1a). As the imidazolyl content was increased, a concomitant increase in size of the nanoparticles was observed. DNA loading further increased the size of the nanoparticles. However, in the presence of 10% serum, the hydrodynamic diameter of samples (PIP-1 to PIP-9) was found to be reduced significantly (Table I). Particularly, in case of PIP-9 nanoparticles, a gradual decrease in the size of the nanoparticles was observed from 83 nm to 25 nm on increasing the concentration of FCS from 5–40%. This reduction of size of the nanoparticles might be due to inhibition of aggregation (Fig. 1b) (30,37). The surface charge of nanoparticles was found to decrease by incorporation of imidazolyl substitution. As imidazolyl substitution was increased, a decrease in zeta potential was observed (Table I). The zeta potential of all nanoparticle formulations also showed similar trend after complexing with DNA, while maintaining the overall positive

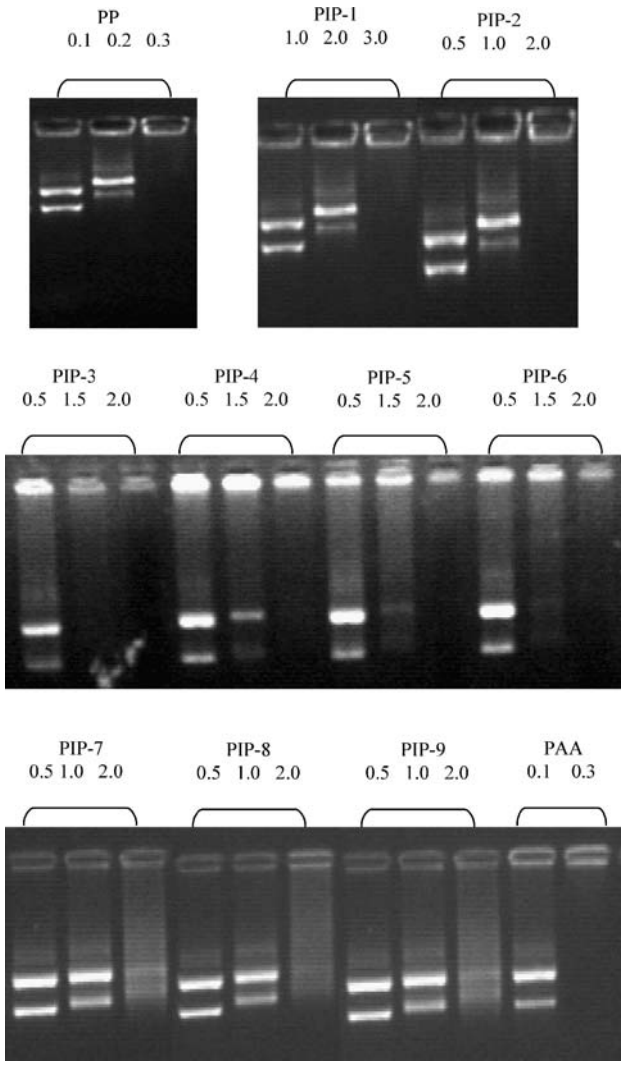

Fig. 2. Gel retardation assay of PIP/DNA complexes. Plasmid DNA (1 μg) was incubated with increasing amounts of nanoparticles in a buffer containing HEPES/NaCl and incubated for 20 min. Samples were electrophoresed through 0.8% agarose gel at 100 V for 45 min. The values mentioned correspond to the amount of nanoparticles (μg) used in a 20 μl reaction to condense pDNA.

charge. The zeta potential of nanoparticles/DNA complexes was found to be negative in FCS. In case of PIP-9, it was observed that on increasing the serum concentration, the zeta potential reduced (Fig. 1b inset).

DNA Complexation

The electrostatic interactions between nanoparticles and pDNA neutralize the negative charge on phosphate group of DNA backbone, thus retarding the DNA mobility under the influence of electric field. The samples of PIP nanoparticles were prepared at different weight ratios and incubated with constant amount of pDNA to determine the optimal concentration of nanoparticles, required for complete retardation of pDNA. PIP-DNA complexes were analyzed on 0.8% agarose gel and visualized by fluorescence of ethidium bromide (Fig. 2). In case of native PAA polymer, retardation was observed at 0.3 μg/μg of pDNA, whereas higher amount of PIP nanoparticles was needed to neutralize the same amount of pDNA. Data showed that increasing the amount of PIP nanoparticles in pDNA complexes resulted in decrease in electrophoretic mobility. PIP nanoparticles completely neutralized the DNA at weight ratio of 2.0 μg/μg in most of the preparations. The amount of PIP nanoparticles required to completely neutralize 1 μg DNA was found to be almost the same in the series, indicating that the degree of imidazolyl substitution did not affect the DNA complexing property of PIP nanoparticles.

Buffering Capacity

Mechanism of DNA delivery by cationic polymers with a pKa around 5.5–6.5 involves rupture of the endosomal compartment and release of DNA into the cytoplasm. The acid-base titration studies were performed to assess the buffering capacity of various nanoparticle formulations. A higher amount of protons required to change in pH of polymer indicated that polymer possess high propensity to be protonated. Fig. 3 shows that the protonation tendency of PIP nanoparticles changed only marginally by imidazolyl substitution as compared to PP nanoparticles. The modification of PAA with imidazolyl does not block the positive charge of PAA rather it delocalizes the charge into the heterocyclic ring of imidazole. Moreover, the buffering range relevant to biological processes involves pH 5–7.5 and we observe that a similar amount of HCl is required for all the members of PIP series for this pH change.

Measurement of DNA Accessibility

It is widely accepted that pDNA should condense into small particles in order to facilitate internalization of nanoparticle by endocytosis. DNA accessibility assay is the simplest approach to monitor free DNA in solutions containing DNA-nanoparticle complexes. As the ratio of nanoparticle was increased in DNA complexes, the accessibility of DNA to interact with EtBr diminished (Fig. 4). The DNA complexes with various PIP preparations at a particular weight ratio were compared in the same assay. It was observed that as the degree of imidazolyl substitution was increased, the amount of free DNA available in the solution

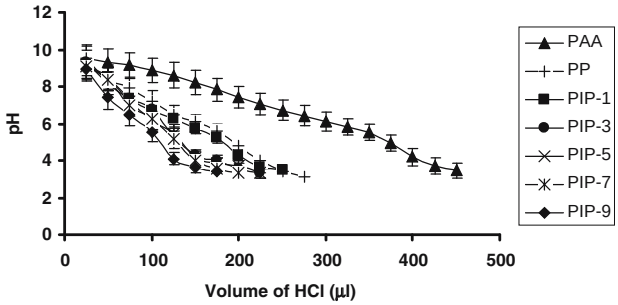

Fig. 3. Buffering capacity of PIP nanoparticles and native PAA. Acid titration curves of aqueous solution of PIP nanoparticles (10 mg/ml) and native PAA (10 mg/ml) were obtained by adding equal aliquots of 0.1 N HCl to nanoparticles dissolved in 150 mM NaCl.

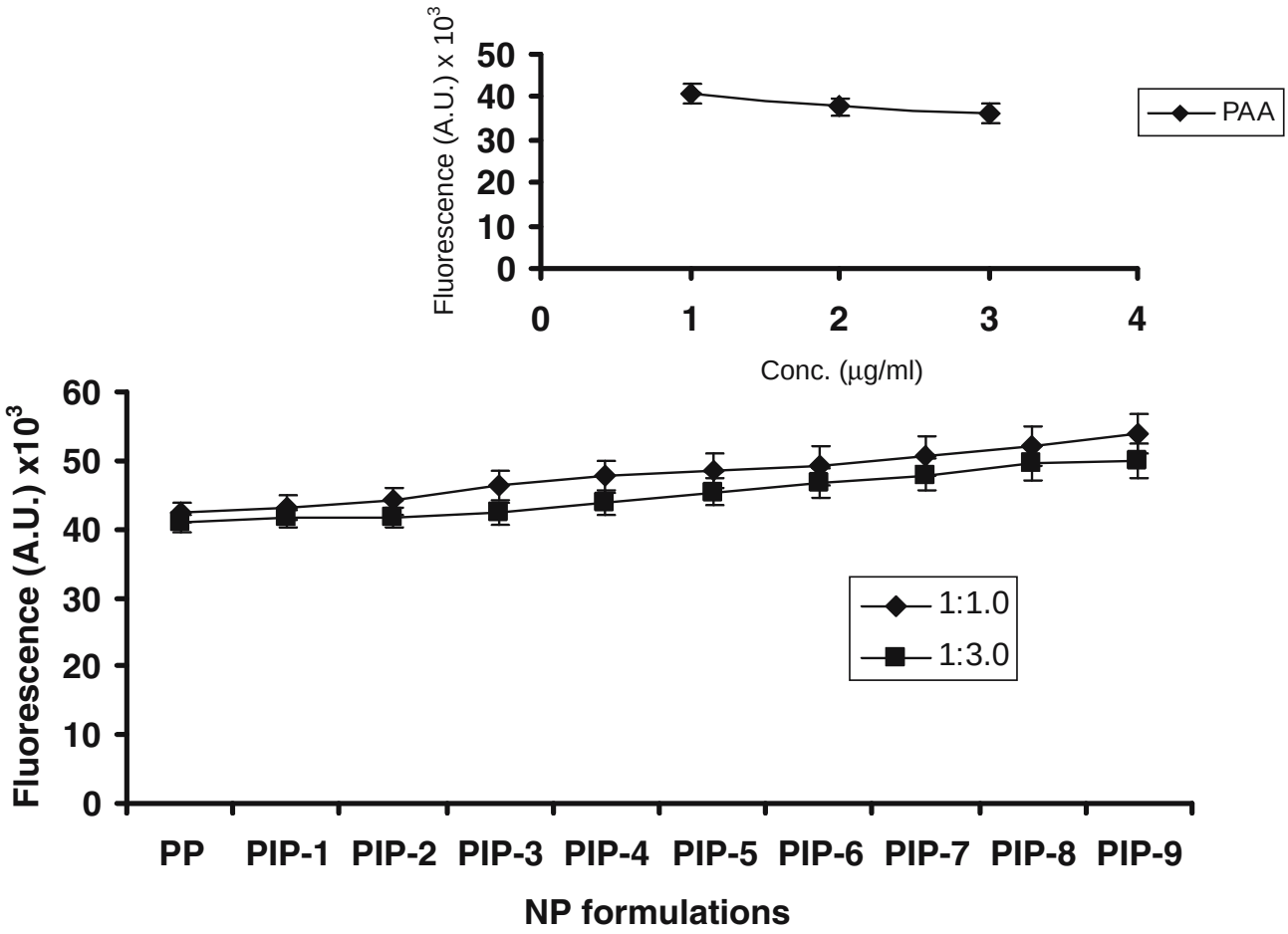

Fig. 4. Measurement of fluorescence intensity (of EtBr) as a function of DNA accessibility in DNA-polymer complexes (w/w ratio 1:1 and 1:3, respectively). In case of PIP/DNA complexes, fluorescence intensity increases with increase in imidazolyl content but decreases with increase in concentration. In case of PAA (*inset*), it decreases with increase in concentration.

also increased (increase in EtBr fluorescence). It appears that the increased imidazolyl substitution results in formation of relatively loose complexes with DNA.

Cell Viability

The cytotoxicity is a major area of concern for novel gene delivery systems. The PIP nanoparticles were examined for their toxicity on COS-1 and HEK293 cell lines using MTT assay. Results (Fig. 5a and b) indicated that toxicity decreased with increase in imidazolyl conjugation to PAA in a non-linear relationship. This further suggested that toxicity level was strongly dependent on degree of substitution of amino groups. Native PAA appeared to be most toxic and the cell viability was found to be ~36%. PP nanoparticles possess higher cell viability compared to native PAA, but lower then imidazolyl substituted nanoparticles. As the imidazolyl substitution increased, the viability reached to 110% (in case of PIP-9 formulation). At weight ratio up to (1:8), PIP nanoparticles were non-toxic compared to PAA. The IC_{50} values of DNA nanoparticles, and PAA were obtained and are compared in Table II. It can be seen that PIP formulations were less toxic than native polymer. It can be concluded that PAA toxicity may be alleviated by imidazolyl modifications.

In Vitro Cell Transfection Studies

The influence of cationic charge density on cytotoxicity and transfection efficiency of PAA was explored. Experiment was performed on COS-1, N2a and HEK293 cells using plasmid containing reporter gene encoding green fluorescence protein (GFP). The weight ratio, greater than the ratio at which complete DNA retardation was observed, was used

Table II. IC_{50} Values for the Various Formulations in the HEK293 Cell Line

Formulation (Weight Ratio)	IC_{50} (μg/ml)
PP (1:2)	6
PIP-1 (1:8)	38
PIP-2 (1:8)	38
PIP-3 (1:8)	38
PIP-4 (1:8)	75
PIP-5 (1:8)	75
PIP-6 (1:8)	75
PIP-7 (1:8)	150
PIP-8 (1:8)	150
PIP-9 (1:8)	150
PAA (1:0.8)	5

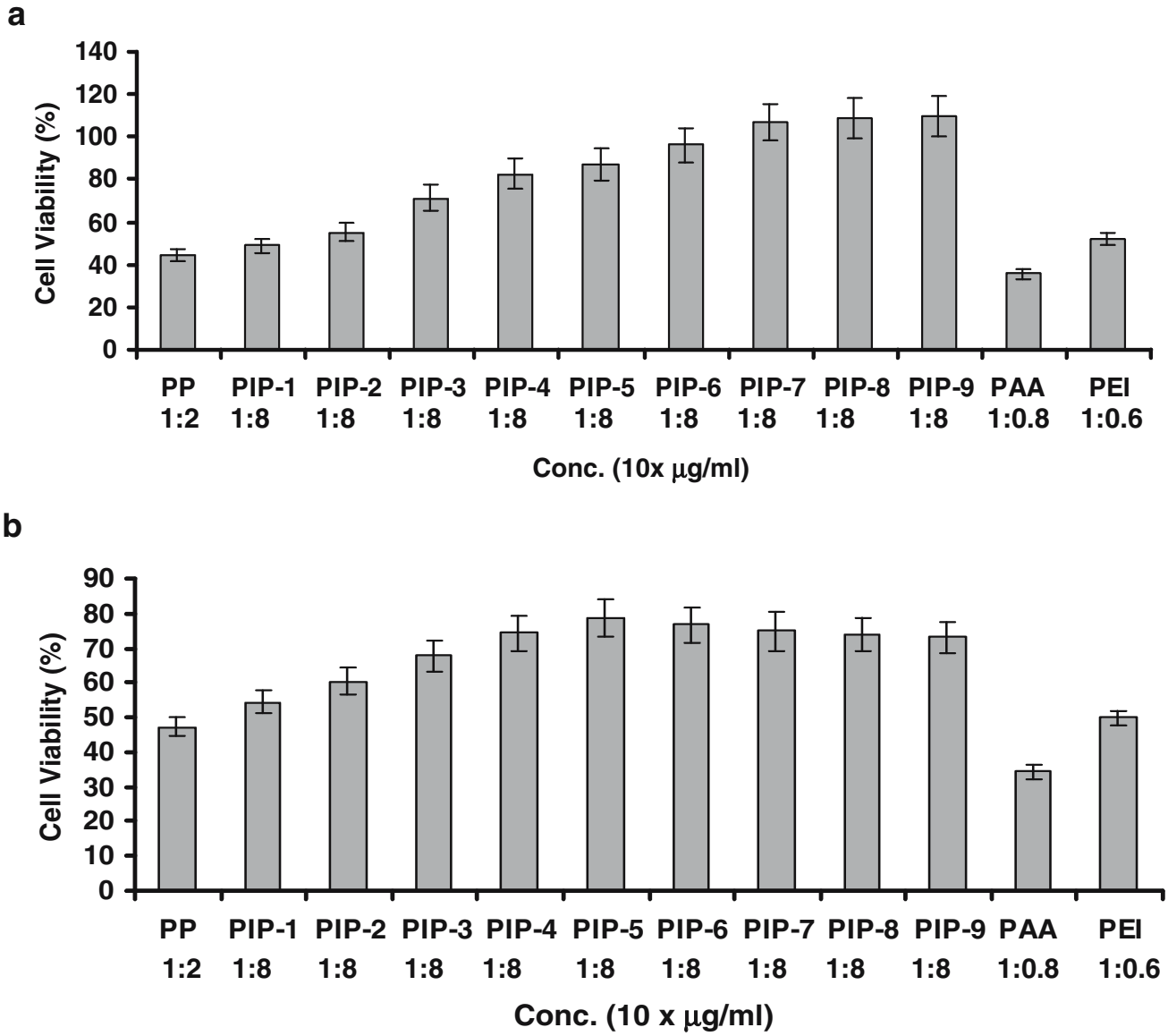

Fig. 5. Cytotoxicity of PIP/DNA complexes on COS-1 and HEK293 cell lines. Cells were treated with PIP/DNA complexes under conditions described in transfection and cytotoxicity was determined by MTT assay. Percent viability of cells is expressed relative to control cells. Each point represents the mean of two independent experiments performed in triplicates for PIP/DNA complexes mediated cytotoxicity at various concentrations. Cytotoxicity associated with PIP/DNA and PIP-9/DNA complexes at maximum transfection efficiency. **a** Cytotoxicity profile of PP, PIP / DNA, PAA and PEI complexes on COS-1 cells. **b** Cytotoxicity profile of PP, PIP / DNA, PAA and PEI complexes on HEK293 cells. **c** Dose dependence curve for cytotoxicity mediated by PAA/DNA and PIP-9/DNA complexes. The concentrations of unmodified PAA used were 0.5,1, 2, 3 μg (per ml) respectively to condense 1 μg pDNA as shown in the inset. **d** Representative dose-dependence curve for cytotoxicity of PIP-5 (w/w ratio 1:8) for calculation of IC_{50} values. The abscissa represents the concentrations (μg/ml) of nanoparticles used to condense 1 μg pDNA.

for transfection. The cells were exposed with various DNA-nanoparticle formulations in 5% dextrose for 3 h. The cells were examined under the fluorescent microscope after 36 h. The transfected cells had fairly high levels of reporter gene expression and appeared to be healthy on microscopic examination (Fig. 6a). The protein expression was quantified spectrofluorimetrically at an excitation wavelength of 488 nm and emission 509 nm. Transfection efficiency was also calculated by counting the cells expressing GFP, and correlated well with the reporter gene expression analysis. Transfection was found to be directly proportional to the content of imidazolyl in PIP nanoparticles. In case of COS-1 cells, transfection efficiency of PAA (which is a poor transfecting agent) was found to be improved by 8–9 folds upon incorporating imidazolyl substitution without addition of any external lysosomotropic agent. Highest transfection was recorded with PIP-9 formulation in case of COS-1 cells and the dose-dependence curve for transfection efficiency is presented (Fig. 6b and c, respectively). Whereas, in N2a and HEK293 cells, PIP-5 formulation gave the maximum

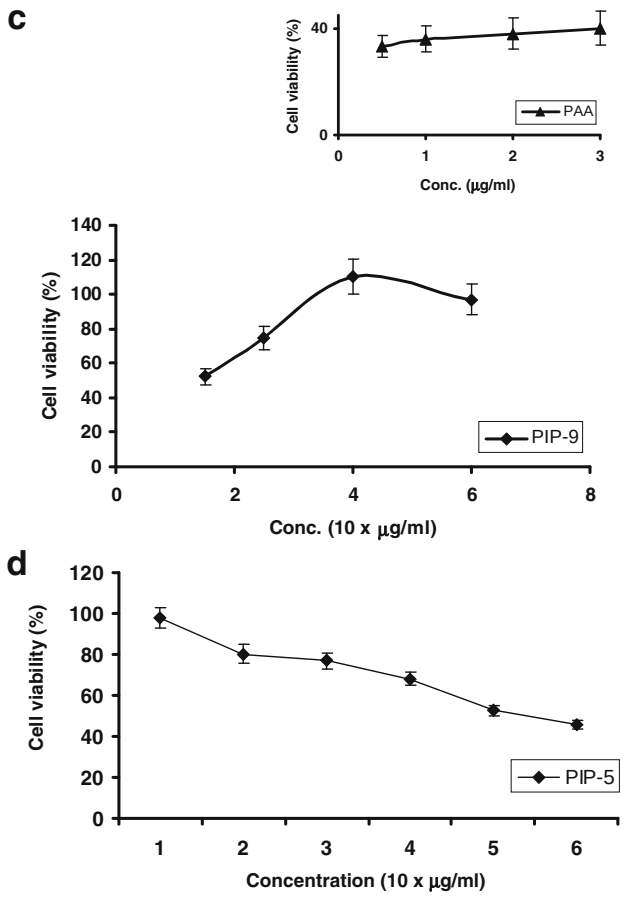

Fig. 5. Continued

expression, i.e. five and four fold, respectively, (Fig. 6d and e). Weight ratios resulting in optimal transfection were also higher in case of PIP nanoparticles compared to native PAA, which were well tolerated by the cells.

DISCUSSION

The most versatile way to enhance the delivery of exogenous DNA into mammalian cells involves complexation with cationic polymers. The complex is internalized, trafficked through the endosomal pathway and finally, resides within the endosome. Hence, several attempts have been made to chemically modify the polycations (i.e. by substituting with imidazolyl or histidine groups) addressing the release from endosome to improve the intracellular gene delivery (38,39).

In this report, library of PAA based nanoparticles was synthesized by varying the concentration of imidazolyl groups and keeping the concentration of PEG cross-linker constant. The PIP nanoparticles (Scheme 1) were designed to improve the sufficient transfection capacity and at the same time reduce the cytotoxicity associated with excess of positive charge. The efficiency of imidazolyl substitution reaction on PAA was ~75–82%, as determined by estimation of amino groups by ninhydrin method. The maximally substituted nanoparticles have 80% replacement of primary amino by imidazolyl moiety and 5% amino groups are involved in cross linking with PEG. The advantages of PEG cross-linker and nanoparticles have been well established in our earlier studies (30,33,40). The substitution was planned in a manner to retain sufficient amount of primary amino groups for DNA interaction and condensation for efficient internalization. The hydrodynamic diameter of various nanoparticles was within the range of 185–230 nm, with a positive surface charge (5.6–13.1 mV) in water. The uniform population of particles (Fig. 1a) retained sufficient positive surface charge to condense DNA (Fig. 2). Particles remained stable and smaller in size in 10% FCS, which is in tune with previous reports (30,37). This is due to adsorptions of anionic serum proteins on the positively charged nanoparticle surfaces, which then prevents hydrophobic contacts between the particles and modify the global surface charge allowing repulsion between particles. The size and surface charge of particles are important factors that modulate their cellular uptake. The positively charged complex can interact with the negatively charged proteoglycans of the cell membrane. The surface charge of nanoparticles was found to decrease upon substitution with protonable imidazolyl moiety (Table I). At neutral pH, imidazole does not carry sufficient charge to electrostatically interact with DNA, thus the availability of positive charge decrease on increasing imidazolyl substitution. The buffering capacity determines the release behavior of DNA-polymer complexes from endosomal compartment, an important step in determining the efficiency of transgene expression. Imidazolyl containing nanoparticles can provide the adequate buffering, avoiding the deleterious effects of the high cationic charge density of PAA due to primary amino groups in the biologically relevant pH range of 5–7.5. The findings were in accordance with previous reports on imidazolyl substitution on PLL (25). All the PIP nanoparticles in the series have similar DNA neutralizing capacity, as indicated in the gel retardation assay (Fig. 3), but the binding affinity for DNA was found to depend on the degree of imidazolyl substitution. As the imidazolyl substitution was increased, the DNA accessibility also improved, indicating formation of relatively loose DNA-nanoparticle complexes. These experiments also suggested that the nanoparticles formed sufficiently stable

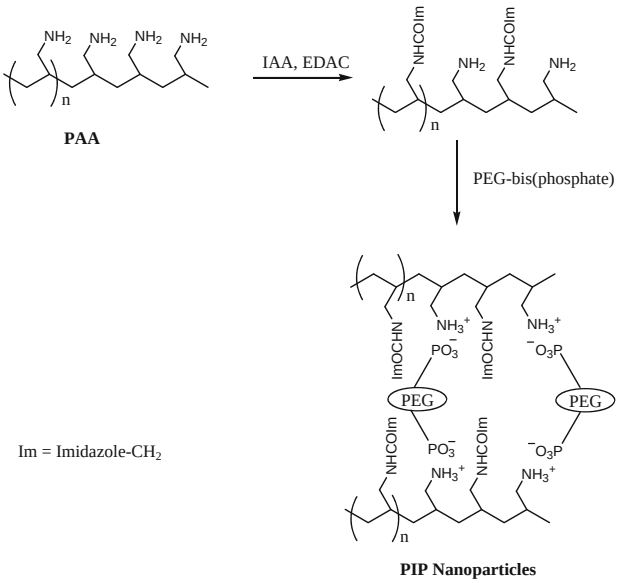

Scheme 1. Schematic representation of PIP nanoparticles synthesis.

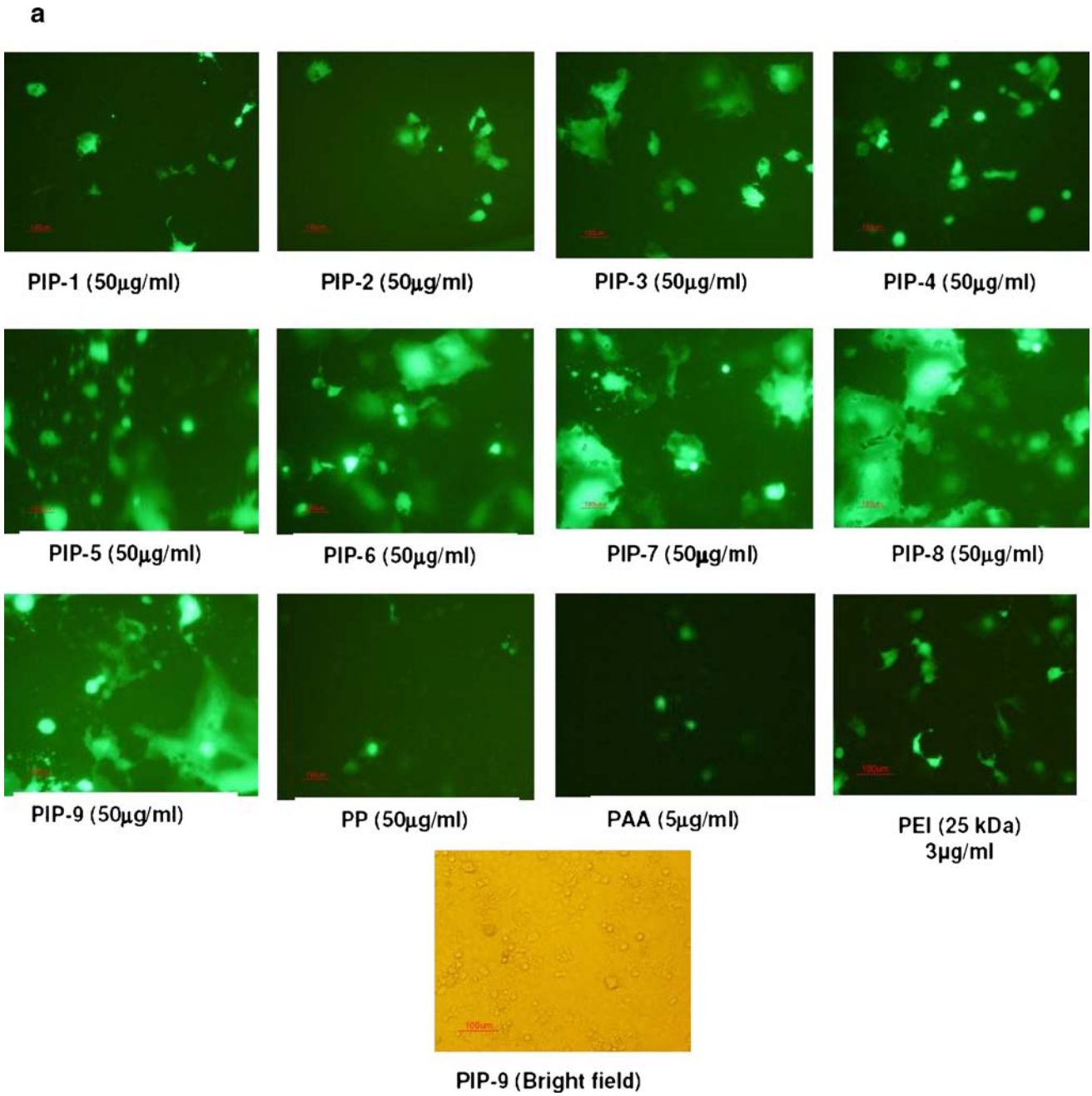

Fig. 6. **a** GFP fluorescence images of COS-1 cells transfected with PIP/DNA complexes. COS-1 cells were incubated with PIP/DNA complexes for 3 h and the expression of GFP was monitored after 36 h. Images were recorded (at 10X magnification). COS-1 cells transfected with respective nanoparticle/DNA complexes as observed under UV, C-F1 epifluorescence filter of fluorescent microscope. **b** The fluorescent intensity of GFP fluorophore in the cell lysate was measured using spectrofluorometer and the results are expressed in terms of A.U./mg total cellular protein. The results represent the mean of two independent experiments performed in triplicates. Transfection efficiency with PAA/DNA (*inset*) and PIP-9/DNA complexes prepared at various weight ratios. The abscissa represents the concentrations (µg/ml) of nanoparticles used to condense 1 µg pDNA. The concentrations of unmodified PAA used were 0.3, 0.5 µg, respectively, to condense 1 µg pDNA. **c** Maximum transfection achieved by PIP-9/DNA complexes in COS-1 cell lines. **d** Maximum transfection achieved by PIP-5/DNA complexes in N2a cell lines **e** Maximum transfection achieved by PIP-5/DNA complexes in HEK293 cell lines. Concentration indicated in the *parenthesis*.

complexes with DNA (Fig. 4). The highlighting feature of the PIP nanoparticles is delivery of DNA inside the cell without diminishing the metabolic functions of the cells as determined by MTT assay. Results revealed that cytotoxicity of PIP nanoparticles decreased with increasing imidazolyl content in the system, in COS-1 and HEK293 cell lines (Fig. 5a and b, respectively). As shown in Fig. 5c, in case of PIP-9 formulation, cell viability was found to be 110% on COS-1 cells, while native PAA showed only 36% survival. In case of HEK293 cells, highest cell viability was observed with PIP-5 formulation (Fig. 5d). Transfection study carried out with reporter gene encoding green fluorescence protein using these PIP nanoparticles was resulted in transfection profiles, as shown in Fig. 6a and b. Transfection with native PAA

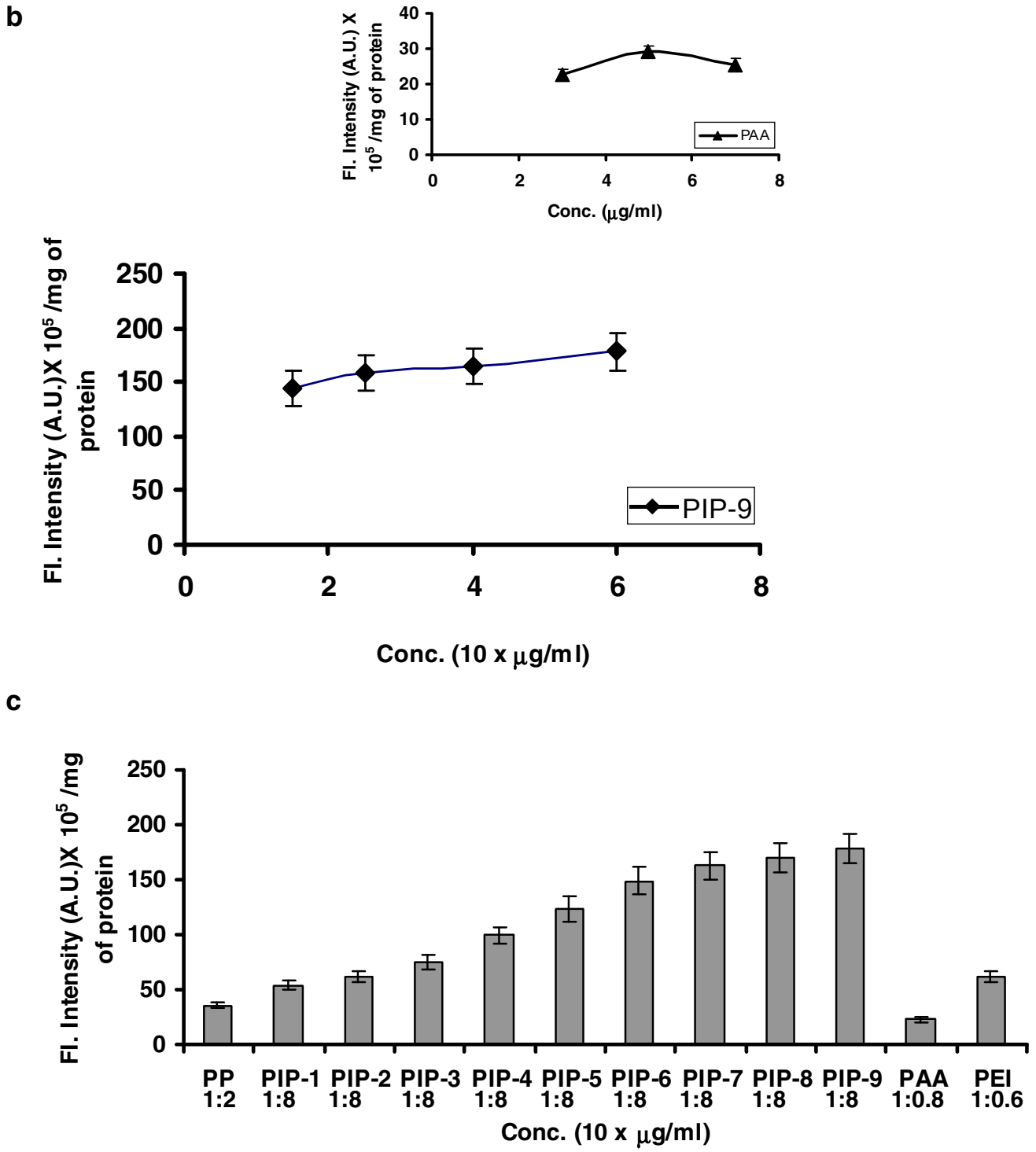

Fig. 6. Continued

resulted in minimal level of GFP fluorescence intensity regardless of DNA: nanoparticle ratio (Fig. 6b inset). This ratio plays a decisive role in the transfection. The reporter gene expression was found to increase on increasing w/w ratio in DNA complexation, which reaches an optimal value and decline afterwards. Beyond optimal transfection efficiency, the toxicity was also evident in the samples, which may be responsible for decreased gene expression. Expression of GFP was also found to increase with increase in imidazolyl substitution. In case of COS-1 cells, gene expression was most pronounced with PIP-7, 8 and 9 members of the series at a weight ratio of 1:8 in all the cases, as shown in Fig. 6c. Modified systems were found to be less toxic than parent polymer and transfection efficiency was found to increase by several orders (~4–9 folds) of magnitude on various cell types (Fig. 6d and e). Results indicated that imidazolyl

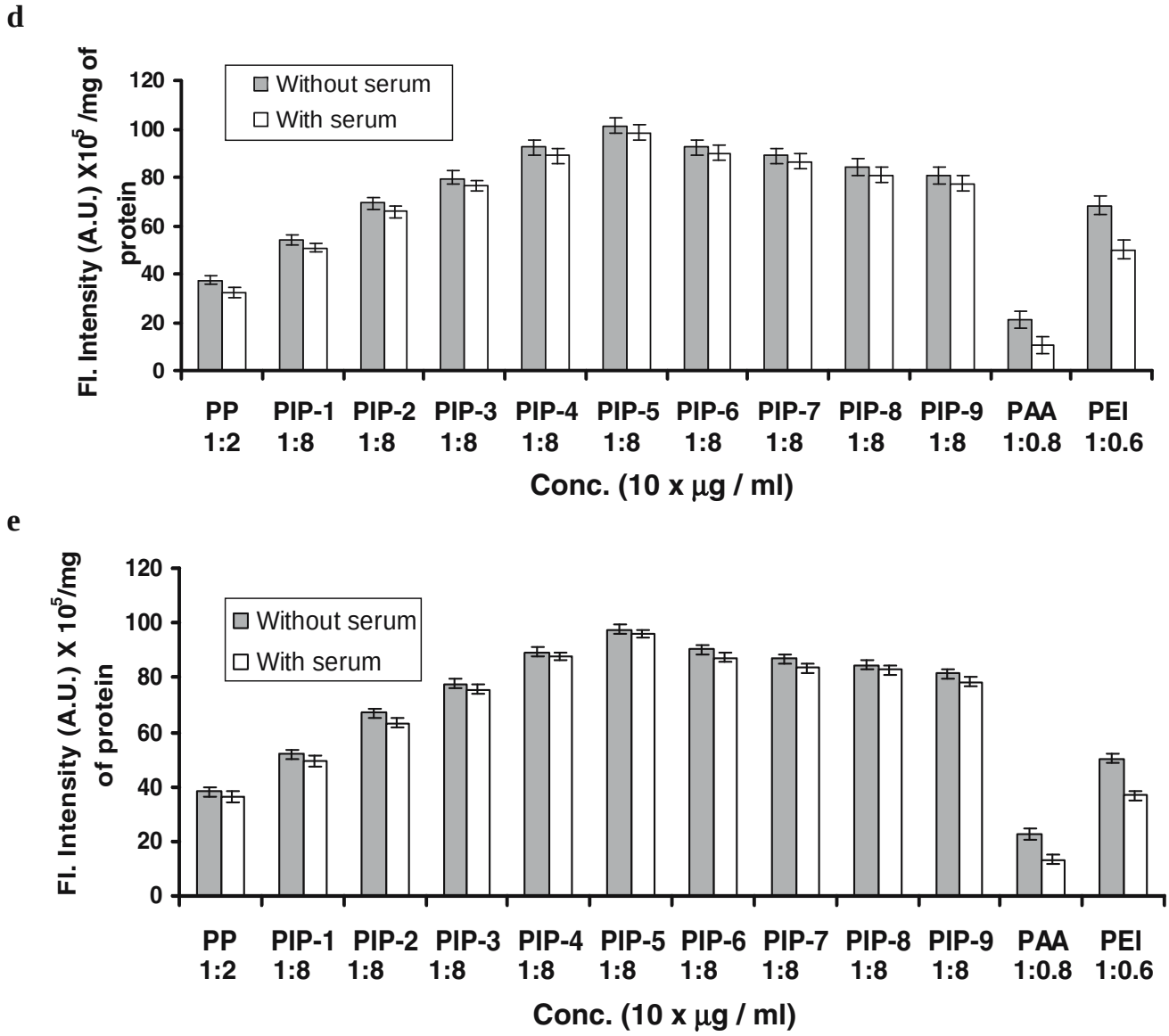

Fig. 6. Continued

moiety plays an important role in improvement of the transfection efficiency of PIP nanoparticles. The imidazolyl group improves the transfection efficiency by virtue of its inherent proton sponge property i.e. efficient release of DNA complex from endosomes. At the same time, the reduced charge density of primary amino groups and delocalized charge in imidazole ring may help in unpacking of DNA and thus result in high levels of gene expression. Moreover, the requirement of external lysosomotropic agent like chloroquine in the transfections by PAA has been completely eliminated by using these systems. Hence, inclusion of imidazolyl moiety in a relatively toxic PAA enhanced the DNA delivery and reduced the toxicity to minimal level.

CONCLUSIONS

In past few years, umpteen reports have been published to eliminate problems like cell uptake, cytotoxicity and endocytosis process. Most strategies focus on modulating the types of amines or cationic groups to enhance the transfection efficiency of polycationic vectors mainly by altering the buffering capacities of the carriers, or by targeted delivery. Efficient non-viral vectors entail a better understanding of the structure-function relationship of the synthesized carrier systems (41). In the present study, an attempt was made to resolve cellular barriers by masking charge of polycations, addressing endosome escape element and unpackaging of DNA. The experiment showed that blocking of primary amino groups of PAA reduced its toxicity index and improved efficiency to carry DNA inside the cell several times. Polycations like PAA have high cationic charge density because of the presence of a number of amino groups on its backbone, which are responsible for its cytotoxicity. The findings bolster the evidence that imidazolyl functionalities help to improve the transfection efficiency of poor transfecting polycations.

ACKNOWLEDGEMENTS

The authors are thankful to Sophisticated Analytical Instrument Facility, Central Drug Research Institute, Lucknow, India and NMR Laboratory, Indian Institute of Technology, Delhi for NMR analysis. Authors (AP, RKK, SP and AS) gratefully acknowledge the Indian Council for Medical Research (ICMR), the Council of Scientific and Industrial Research (CSIR) and the University Grant Commission (UGC), respectively, for providing financial support.

REFERENCES

1. E. Piskin, S. Dincer, and M. Turk. Gene delivery: intelligent but just at the beginning. *J. Biomater. Sci., Polym. Ed.* **15**:1181–1202 (2004).
2. D. Luo and W. M. Saltzman. Synthetic DNA delivery systems. *Nat. Biotechnol.* **18**:33–37 (2000).
3. C. M. Cavazzana, S. B. Hacein, G. B. deSaint, F. Gross, E. Yvon, P. Nusbaum, P. Selz, C. Hue, S. Certain, J. L. Casanova, P. Bousso, F. L. Deist, and A. Fischer. Gene therapy of human severe combined immunodeficiency (SCID)-X1 disease. *Science* **288**:669–672 (2000).
4. C. M. Liu, D. P. Liu, W. J. Dong, and C.-C. Liang. Retrovirus vector-mediated stable gene silencing in human cell. *Biochem. Biophys. Res. Commun.* **313**:716–720 (2004).
5. D. T. Curiel, S. Agrawal, E. Wagner, and M. Cotton. Adenovirus enhancement of transferrin-polylysine-mediated gene delivery. *Proc. Natl. Acd. Sci. USA* **88**:8850–8854 (1991).
6. A. Fasbender, J. Zabner, M. Chillon, T. O. Moninger, A. P. Puga, B. L. Davidson, and M. J. Welsh. Complexes of adenovirus with polycationic polymers and cationic lipids increase the efficiency of gene transfer *in vitro* and *in vivo*. *J. Biol. Chem.* **272**:6479–6489 (1997).
7. P. L. Felgner, T. R. Gadek, M. Holm, R. Roman, H. W. Chan, M. Wenz, J. P. Northrop, G. M. Ringold, and M. Danielsen. Lipofection: a highly efficient, lipid-mediated DNA-transfection procedure. *Proc. Natl. Acad. Sci. USA* **84**:7413–7417 (1987).
8. M. A. Ilies, B. H. Johnson, F. Makori, A. Miller, W. A. Seitz, F. B. Thompson, and A. T. Balaban. Pyridinium cationic lipids in gene delivery: an *in vitro* and *in vivo* comparison of transfection efficiency versus a tetraalkylammonium congener. *Arch. Biochem. Biophys.* **435**:217–226 (2005).
9. S. Simoes, A. Filipe, H. Faneca, M. Mano, N. Penacho, N. Duzgunes, and M. P. Limade. Cationic liposomes for gene delivery. *Expert Opin. Drug Deliv.* **2**:237–254 (2005).
10. S. I. Kim, S. K. Lee, Y. M. Park, Y. B. Lee, S. C. Shin, K. C. Lee, and I. J. Oh. Physicochemical characterization of poly(L-lactic acid) and poly(D,L-lactide-co-glycolide) nanoparticles with polyethylenimine as gene delivery carrier. *Int. J. Pharm.* **298**:255–262 (2005).
11. R. G. Crystal. Transfer of genes to human: early lessons and obstacles to success. *Science* **270**:404–410 (1995).
12. P. L. Felgner, Y. Barenholz, J. P. Behr, S. H. Cheng, P. Cullis, L. Huang, J. A. Jessee, L. Seymour, F. Szoka, A. R. Thierry, E. Wagner, and G. Wu. Nomenclature for synthetic gene delivery systems. *Hum. Gene Ther.* **20**:511–512 (1997).
13. S. Hacein-Bey-Abina, C. Von Kalle, M. Schmidt, M. P. McCormack, N. Wulffraat, P. Leboulch, A. Lim, C. S. Osborne, R. Pawliuk, E. Morillon, R. Sorensen, A. Forster, P. Fraser, J. I. Cohen, G. de Saint Basile, I. Alexander, U. Wintergerst, T. Frebourg, A. Aurias, D. Stoppa-Lyonnet, S. Romana, I. Radford-Weiss, F. Gross, F. Valensi, E. Delabesse, E. Macintyre, F. Sigaux, J. Soulier, E. Leiva, M. Wissler, C. Prinz, T. H. Rabbitts, F. Le Deist, A. Fischer, and M. Cavazzana-Calvo. LMO2-associated clonal T-cell proliferation in two patients after gene therapy for SCID-X1. *Science* **302**:400–401 (2003).
14. J.-P. Behr. The proton sponge: a trick to enter cells the viruses did not exploit. *Chimia* **51**:34–36 (1997).
15. P. Chollet, M. C. Favrot, A. Hurbin, and J. L. Coll. Side-effects of a systemic injection of linear polyethylenimine–DNA complexes. *J. Gene Med.* **4**:84–91 (2002).
16. W. T. Godbey, K. K. Wu, and A. G. Mikos. Poly(ethylenimine) and its role in gene delivery. *J. Control. Release* **60**:149–160 (1999).
17. S. Nimesh, R. Kumar, and R. Chandra. Novel polyallylamine–dextran sulfate–DNA nanoplexes: highly efficient non-viral vector for gene delivery. *Int. J. Pharm.* **320**:143–149 (2006).
18. O. Boussif, T. Delair, C. Brua, L. Veron, A. Pavirani, and H. V. Kolbe, O. Synthesis of polyallylamine derivative and their use as a gene transfer vectors *in vitro*. *Bioconjug. Chem.* **10**:877–883 (1999).
19. Y. H. Choi, F. Liu, J. S. Kim, Y. K. Choi, J. S. Park, and S. W. Kim. Polyethylene glycol-grafted-polylysine as polymeric gene carriers. *J. Control. Release* **54**:39–48 (1998).
20. M. T. Peracchia, C. Vauthier, D. Desmaele, A. Gulik, C. Dedieu, M. demoy, J. Angelo, and P. Couvreur. Pegylated nanoparticles from a novel methoxypolyethylene-glycol cyanoacrylate-hexadecyl amphiphile copolymer. *Pharm. Res.* **15**:550–556 (1990).
21. C. H. Ahn, S. Y Chae, Y. H. Bae, and S. W. Kim. Synthesis of biodegradable multi-block copolymers of poly(L-lysine) and poly(ethylene glycol) as a non-viral gene carrier. *J. Control. Release* **97**:567–574 (2004).
22. M. L. Forrest, G. E. Meister, J. T. Koerber, and D. W. Pack. Partial acetylation of polyethylenimine enhances *in vitro* gene delivery. *Pharm. Res.* **21**:365–371 (2004).
23. W. Tiyaboonchai, J. Woiszwillo, and C. R. Middaugh. Formulation and characterization of DNA–polyethyleneimine-dextran sulfate nanoparticles. *Eur. J. Pharm. Sci.* **19**:191–202 (2003).
24. M. L. Forrest, N. Gabrielson, and D. W. Pack. Cyclodextrin-polyethylenimine conjugates for targeted *in vitro* gene delivery. *Biotechnol. Bioeng.* **89**:416–423(2005).
25. D. J. Chen, B. S. Majors, A. Zelikin, and D. Putnam. Structure-function relationship of gene delivery vectors in a limited polycation library. *J. Control. Release* **103**:273–293 (2005).
26. D. W. Pack, D. Putnam, and R. Langer. Design of imidazole-containing endosomolytic biopolymers for gene delivery. *Biotechnol. Bioeng.* **67**:217–223 (2000).
27. R. M. Bello and P. Midoux. Histidylated polylysine as DNA vector: elevation of the imidazole protonation and reduced cellular uptake without change in the polyfection efficiency of serum stabilized negative polyplexes. *Bioconjug. Chem.* **12**:92–99 (2001).
28. P. Dubruel, B. Christiaens, M. Rosseneu, J. Vandekerckhove, J. Grooten, V. Goossens, and E. Schacht. Buffering properties of cationic polymethacrylates are not the only key to successful gene delivery. *Biomacromolecules* **5**:379–388 (2004).
29. T. H. Kim, J. E. Ihm, Y. J. Choi, J. W. Nah, and C. S. Cho. Efficient gene delivery by urocanic acid-modified chitosan. *J. Control. Release* **93**:389–402 (2003).
30. A. Swami, A. Aggarwal, A. Pathak, S. Patnaik, P. Kumar, Y. Singh, and K. C. Gupta. Imidazolyl-PEI modified nanoparticles for enhanced gene delivery. *Int. J. Pharm.* (2007) (In press).
31. J. Suh, H.-J. Paik, and B. K. Hwang. Ionization of Poly(ethylene) and Poly(allylamine) at various pH's. *Bioorg. Chem.* **22**:318–327 (1994).
32. H. Eliyahu, A. Makovitzki, T. Azzam, A. Zlotkin, A. Joseph, D. Gazit, Y. Barenholz, and A. J. Domb. Novel dextran-spermine conjugates as transfecting agents: comparing water-soluble and micellar polymers. *Gene Ther.* **12**:494–503 (2005).
33. S. Nimesh, A. Goyal, V. Pawar, S. Jayaraman, P. Kumar, R. Chandra, Y. Singh, and K. C. Gupta. Polyethylenimine nanoparticles as efficient transfecting agents for mammalian cells. *J. Control. Release* **110**:457–468 (2006).
34. P.-Y. Yeh, P. Kopeckova, and J. Kopecek. Biodegradable and pH sensitive hydrogels: synthesis by crosslinking of N,N-dimethylacrylamide copolymer precursors. *J. Polym. Sci., A, Polym. Chem.* **32**:1627–1637 (1994).
35. D. Putnam, C. A. Gentry, D. W. Pack, and R. Langer. Polymer-based gene delivery with low cytotoxicity by a unique balance of side-chain termini. *Proc. Natl. Acad. Sci. USA* **98**:1200–1205 (2001).
36. M. Glodde, S. R. Sirsi, and G. J. Lutz. Physiochemical properties of low and high molecular weight poly(ethylene glycol)-grafted

poly(ethyleneimine) copolymers and their complexes with oligonucleotides. *Biomacromolecules* **7**:347–356 (2006).
37. M. B. Roufai and P. Midoux. Histidylated polylysine as DNA vector: elevation of the imidazole protonation and reduced cellular uptake without change in the polyfection efficiency of serum stabilized negative polyplexes. *Bioconjug. Chem.* **12**:92–99 (2001).
38. J. E. Ihm, Ki-Ok Han, C. S. Hwang, J. H. Kang, K.-D. Ahn, I.-K. Han, D. K. Han, J. A. Hubbell, and C.-S. Su. Poly (4-vinylimidazole) as nonviral gene carrier: *in vitro* and *in vivo* transfection. *Acta Biomaterialia* **1**:165–172 (2005).
39. E. S. Lee, H. J. Shin, K. Na, and Y. H. Bae. Poly (L-histidine)-PEG block copolymer micelles and pH-induced destabilization. *J. Control. Release* **90**:363–374 (2003).
40. S. Patnaik, A. Aggarwal, A. Goel, M. Ganguli, N. Saini, Y. Singh, and K. C.Gupta. PEI-alginate nanocomposites as efficient *in vitro* gene transfection agents. *J. Control. Release* **114:**398–409 (2006).
41. M. Koping-Hoggard, I. Tubulekas, H. Guan, K. Edwards, M. Nilsson, K. M. Varum, and P. Artursson. Chitosan as a nonviral gene delivery system. Structure-property relationships and characteristics compared with polyethylenimine *in vitro* and after lung administration *in vivo*. *Gene Ther.* **8**:1108–1121 (2001).